

Anion $A^- \bullet HX$ Clusters with Reduced Electron Binding Energies: Proton vs Hydrogen Atom Relocation upon Electron Detachment

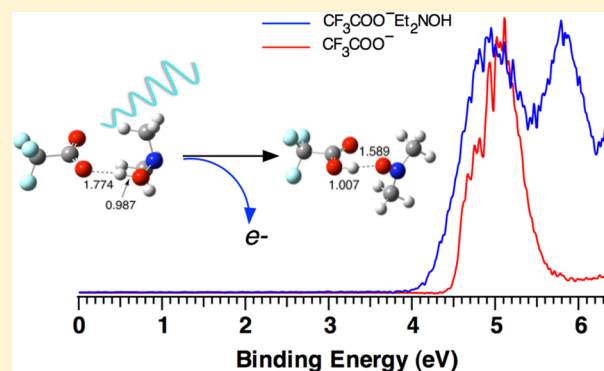
Xue-Bin Wang^{*,‡} and Steven R. Kass^{*,†}

[†]Department of Chemistry, University of Minnesota, Minneapolis, Minnesota 55455, United States

[‡]Physical Sciences Division, Pacific Northwest National Laboratory, P.O. Box 999, MS K8-88, Richland, Washington 99352, United States

S Supporting Information

ABSTRACT: Clustering an anion with one or more neutral molecules is a stabilizing process that enhances the oxidation potential of the complex relative to the free ion. Several hydrogen bond clusters (i.e., $A^- \bullet HX$, where $A^- = H_2PO_4^-$ and $CF_3CO_2^-$ and $HX = MeOH$, $PhOH$, and Me_2NOH or Et_2NOH) are examined by photoelectron spectroscopy and M06-2X and CCSD(T) computations. Remarkably, these species are experimentally found to have adiabatic detachment energies that are smaller than those for the free ion and reductions of 0.47 to 1.87 eV are predicted computationally. Hydrogen atom and proton transfers upon vertical photodetachment are two limiting extremes on the neutral surface in a continuum of mechanistic pathways that account for these results, and the whole gamut of possibilities are predicted to occur.

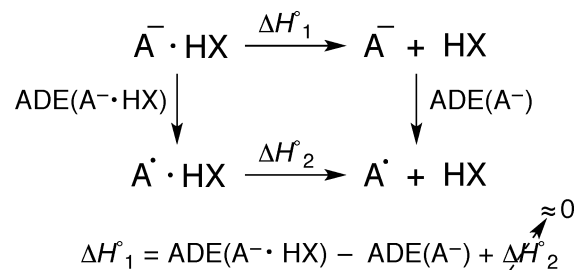


INTRODUCTION

Gas phase ionic clusters are stabilized by ion–neutral interactions because they disperse the charge over a larger volume than in the free ion and thereby lower the energy of the system. When hydrogen bonds are involved, anionic $A^- \bullet HX$ complexes are typically stabilized by ~ 20 – 25 kcal mol⁻¹.¹ This usually results in diminished reactivity of the complex relative to the free anion² and always leads to reduced proton affinities (PAs) and increased adiabatic electron detachment energies (ADEs) (i.e., oxidation potentials);³ the one exception is MI^{*-} ($M = Li$ or Cs), which have bigger ADEs than their water complexes.⁴ This is due to a change in the electronic states of the neutral and anionic alkali iodides and stronger interactions of the former species with water.

Photoelectron spectroscopy is often used to obtain reliable estimates of cluster energies (ΔH_1°) because $ADE(A^- \bullet HX) - ADE(A^-)$ (i.e., ΔADE) is generally a good measure of this quantity given that the interactions in $A^\bullet \bullet HX$ are much weaker than those in the ionic complex, and typically are small (Scheme 1).⁵ Recently, $PhOH \bullet Cl^-$ was found to have a ΔADE that is only half of the dissociation energy (i.e., $\Delta ADE = 12.4$ vs $\Delta H_1^\circ = 26.0$ kcal mol⁻¹), however, and this was attributed to a larger than normal $OH \bullet Cl^\bullet$ interaction due to the large 15.1 kcal mol⁻¹ difference in the H–Cl and PhO–H homolytic bond dissociation enthalpies (i.e., BDEs).⁶ In this report, cluster anions with larger BDE differences are examined and hydrogen bonds are found to lower their oxidation potentials and reduce the ADE of $A^- \bullet HX$ to below the value for A^- in some cases. This is the result of what can be viewed as

Scheme 1. Thermodynamic Cycle Relating the Cluster Energy ΔH_1° to $ADE(A^- \bullet HX) - ADE(A^-)$ (ΔADE) and the Small Radical Stabilization Energy ΔH_2°



proton or hydrogen atom transfer upon vertical photodetachment to the neutral surface, and though both of these individual processes appear to take place, they are limiting extremes in a continuum of mechanistic possibilities.

EXPERIMENTAL SECTION

Photoelectron Spectroscopy. Electrospray ionization of aqueous methanolic solutions of NaH_2PO_4 and CF_3CO_2Na ($\sim 10^{-3}$ M) afforded the corresponding $(M - Na)^-$ and $(M - Na + CH_3OH)^-$ anions. Addition of a methanolic solution of diethylhydroxylamine to both of these mixtures was used to produce the Et_2NOH clusters whereas the $PhOH$ complexes were formed from aqueous acetonitrile solutions of the sodium salts and phenol. Photoelectron spectra of the

Received: October 23, 2014

Published: November 19, 2014

eight resulting ions were obtained at 20 K using an ArF excimer laser at 193 nm (6.424 eV) with an instrument that was previously described.⁷ This apparatus has a 5.2 m flight tube for collecting and analyzing the photoelectrons, and the resulting data were calibrated by recording the known spectra of I^{-8} and $Cu(CN)_2^{-9}$. In all instances, the laser was operated at 20 Hz to enable shot-to-shot background correction of the observed intensities, and the resulting spectra have a resolution of ~ 50 meV for electrons with kinetic energies of ~ 2.5 eV.

Computations. Geometry optimizations and vibrational frequencies for each structure were determined using M06-2X¹⁰ and the aug-cc-pVTZ basis set.¹¹ These calculations were performed at the Minnesota Supercomputer Institute for Advanced Computational Research using Gaussian 09.¹² Zero-point energies (ZPEs) and thermal corrections (TCs) for the enthalpies to 298 K were obtained by using unscaled vibrational frequencies. CCSD(T)/aug-cc-pVTZ single point energies were also computed for the smaller species (Supporting Information Table S1).¹³ Optimized anion structures provided the starting geometries for the radical calculations. For the $H_2PO_4^-/Me_2NOH$ cluster, the geometry optimization was carried out with and without computing the second derivatives of the Hessian matrix at each step of the process. This led to two different conformers, but the hydroxyl hydrogen migrated to the dihydrogen phosphate moiety in both cases.

RESULTS AND DISCUSSION

To computationally and experimentally probe $A^- \bullet HX$ complexes that might have negative $\Delta ADEs$ (i.e., hydrogen bonded clusters where $ADE(A^-) > ADE(A^- \bullet HX)$), species derived from $H-X$ and $H-A$ that have large heterolytic deprotonation enthalpy (ΔH_{acid}°) and homolytic BDE differences (i.e., $\Delta \Delta H_{acid}^\circ$ and ΔBDE) are desired. The former criterion is to ensure that the cluster ions adopt a $A^- \bullet HX$ structure rather than a $AH \bullet X^-$ geometry, whereas the latter one provides the thermodynamic driving force for lowering the oxidation potential of the complex. That is, if the removal of an electron is coupled to a hydrogen shift, then the ADE of the cluster ion will be reduced by the value for ΔBDE . Consequently, the conjugate bases of strong acids (H_3PO_4 and CF_3CO_2H) were used for A^- because they also have strong O–H BDEs. For HX , Me_2NOH , $PhOH$, and $MeOH$ were employed because their BDEs range from 74–105 kcal mol⁻¹ and this affords $\Delta BDEs$ of ~ 10 –40 kcal mol⁻¹ (Table 1).^{14–19}

Density functional theory geometry optimizations and vibrational frequencies of the individual HA and HX acids, their conjugate bases and corresponding radicals were carried out with the M06-2X functional and the aug-cc-pVTZ basis set as this approach generally performs as well or better than the more common B3LYP functional.^{10,11} Coupled cluster calculations with triple excitations on the M06-2X optimized structures¹³ were also carried out with the same basis set (i.e., CCSD(T)/aug-cc-pVTZ single point energies) and the resulting ΔH_{acid}° , ADE, and BDE values are given in Table 1. Both theoretical methods provide predictions that are in good accord with each other and the available experimental data.

The same two computational approaches were employed for $H_2PO_4^- \bullet MeOH$ and $CF_3CO_2^- \bullet MeOH$ but only M06-2X calculations were carried out on the larger cluster anions given the good accord between these two procedures (Figure 1). Neutral complexes were initially computed using the optimized geometries of the negatively charged clusters to obtain the vertical detachment energies (VDEs), and then they were fully optimized to provide the ADEs (Figure 2 and Table 2); all of the xyz coordinates are given in Table S1 in the Supporting Information.

Table 1. Computed M06-2X and CCSD(T) Acidities, BDEs and ADEs for a Series of Oxygen Acids and Their Conjugate Bases

compd (HX)		calc ^a	expt
H_3PO_4	$\Delta H_{acid}^\circ(HX)$	328.5 [329.0]	330.5 ± 5^b
	$ADE(X^-)$	4.36 [4.30]	4.57 ± 0.10^c
	BDE(HX)	116.7 [114.7]	122 ± 6
CF_3CO_2H	$\Delta H_{acid}^\circ(HX)$	321.9 [324.4]	323.3 ± 2.9^d
	$ADE(X^-)$	4.66 [4.53]	
	BDE(HX)	116.9 [115.3]	
$PhOH$	$\Delta H_{acid}^\circ(HX)$	348.2 [349.5]	348.0 ± 1.0^e
	$ADE(X^-)$	2.33 [2.27]	2.253 ± 0.006^f
	BDE(HX)	89.5 [88.4]	86.3 ± 1.0^e
$MeOH$	$\Delta H_{acid}^\circ(HX)$	381.3 [382.4]	381.9 ± 0.5^g
	$ADE(X^-)$	1.47 [1.47]	1.5690 ± 0.0019^h
	BDE(HX)	102.8 [103.0]	104.6 ± 0.7^g
Me_2NOH	$\Delta H_{acid}^\circ(HX)$	376.2 [376.3]	
	$ADE(X^-)$	0.34 [0.47]	
	BDE(HX)	71.7 [73.6]^i	

^aAcidities and bond energies are at 298 K and in kcal mol⁻¹ whereas ADEs are at 0 K and in eV. CCSD(T) values are given in brackets.

^bRef 3. ^cRef 14. ^dAverage of two values (322.8 and 323.8 ± 2.9 kcal mol⁻¹) from ref 3. ^eRef 15. ^fRef 16. ^gRef 17. ^hRef 18. ⁱA recommended value of 72.7 kcal mol⁻¹ based upon the average of a G3 and CBS-Q prediction previously was reported. See ref 19.

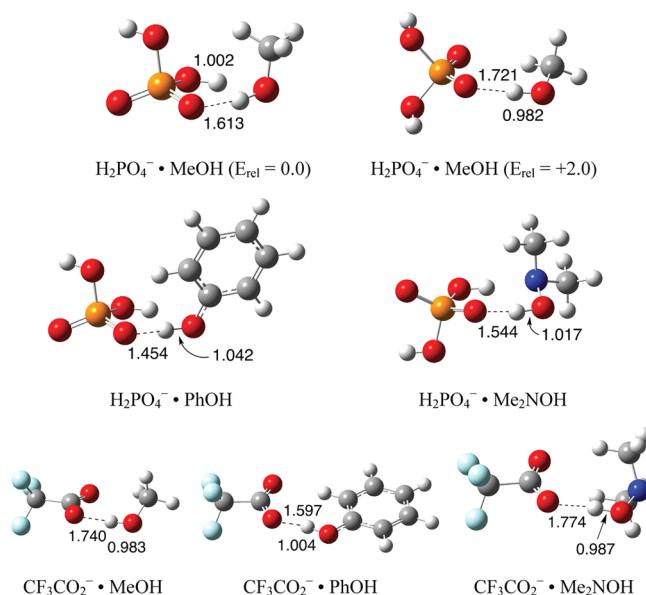


Figure 1. Optimized M06-2X/aug-cc-pVTZ cluster anion geometries; relative energies are in kcal mol⁻¹.

Hydrogen shifts were observed in all of the radical complexes except for dihydrogen phosphate–methanol, which has the neutral partner with the strongest O–H bond and a barrier for the hydrogen shift. There is a slightly higher energy conformer of the anion cluster (+2.0 kcal mol⁻¹), however, that leads to a C–H shift in the corresponding radical. Given that BDE($HOCH_2-H$) = 96.1 ± 0.2 kcal mol⁻¹²⁰ and this value is 8.5 kcal mol⁻¹ smaller than for the O–H bond, this suggests that ΔBDE needs to be $\geq \sim 15$ kcal mol⁻¹ in dihydrogen phosphate clusters for the hydrogen atom to shift in the radical (i.e., the average of $\Delta BDE((HO)_2P(O)O-H - HOCH_2-H)$ and $\Delta BDE((HO)_2P(O)O - H - CH_3O-H)$); the corresponding value for the $CF_3CO_2^-$ clusters apparently is smaller as the O–

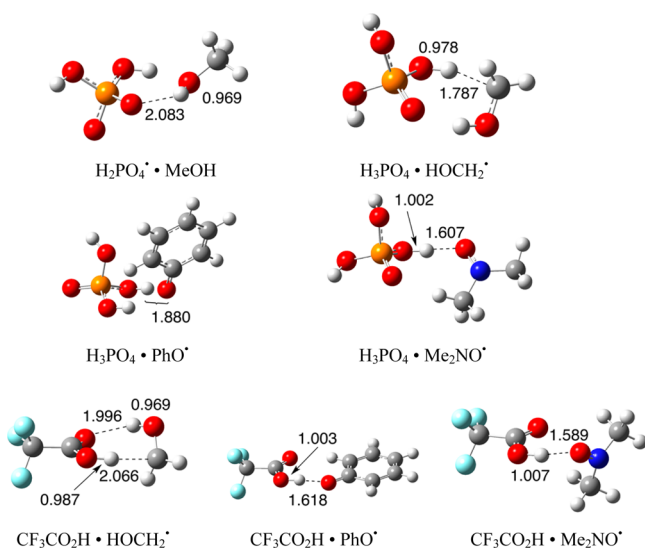


Figure 2. Optimized M06-2X/aug-cc-pVTZ radical cluster geometries.

Table 2. Computed and Experimental VDEs and ADEs in eV

Ion	calc ^a		expt ^b	
	VDE	ADE	VDE	ADE
H ₂ PO ₄ ⁻	5.20 (5.10)	4.36 (4.30)	5.1	4.55 ^{c,d}
H ₂ PO ₄ ⁻ • MeOH	5.67 [5.70] ^e	4.63 (4.56) [3.60 (3.66)] ^e	5.7	≤4.9
H ₂ PO ₄ ⁻ • PhOH	5.10	3.89	5.0	≤4.0
H ₂ PO ₄ ⁻ • Me ₂ NOH	5.11	2.77	5.0	≤3.95
CF ₃ CO ₂ ⁻	5.22 (4.93)	4.66 (4.53)	5.0	4.45 ^f
CF ₃ CO ₂ ⁻ • MeOH	5.86	3.97 (3.96)	5.8	≤5.0
CF ₃ CO ₂ ⁻ • PhOH	4.98	3.91	5.1	≤4.2
CF ₃ CO ₂ ⁻ • Me ₂ NOH	4.90	2.79	4.9	≤3.9

^aM06-2X and CCSD(T) (in parentheses) energies. ^bExperimental uncertainties are estimated to be ±0.1 eV. ^cRef 14 gives 4.57 eV. ^dThe ADE of each free anion was obtained by drawing a straight line along the rising edge of each spectrum and adding the instrumental resolution to the crossing point with the binding energy axis. ^eThe results for the less stable conformer mentioned in the text are given in brackets. ^fAn estimated value of 4.46 ± 0.18 eV for this quantity is reported on the NIST Web site (ref 3).

H hydrogen relocates in the methanol complex in this case. As for the energetics, the VDEs of all six A⁻ • HX clusters are predicted to be larger than the ADEs of the free ion (i.e., H₂PO₄⁻ or CF₃CO₂⁻) as expected. The ADEs are all *less* than the values for the free ions except for H₂PO₄⁻ • MeOH because there is no hydrogen shift from the lowest energy conformer in this case. The slightly higher energy structure (+2.0 kcal mol⁻¹, Figure 1) does give a radical that undergoes a hydrogen shift from the carbon atom, and consequently, this species has a reduced ADE below the value for H₂PO₄⁻. The computed ADE reductions for the clusters listed in Table 2 range from 0.47–1.87 eV (i.e., 11–43 kcal mol⁻¹), indicating that ion clustering via hydrogen bond formation can significantly lower oxidation potentials and energetically facilitate electron transfer.

Low temperature photoelectron spectra of A⁻ • HX, where A⁻ = H₂PO₄⁻ or CF₃CO₂⁻ and HX = MeOH, PhOH, and Et₂NOH (not the smaller dimethyl analog that was used in the

computations) were obtained at 20 K with a ArF excimer laser at 193 nm (6.424 eV, Figures 3 and 4).⁷ The vertical

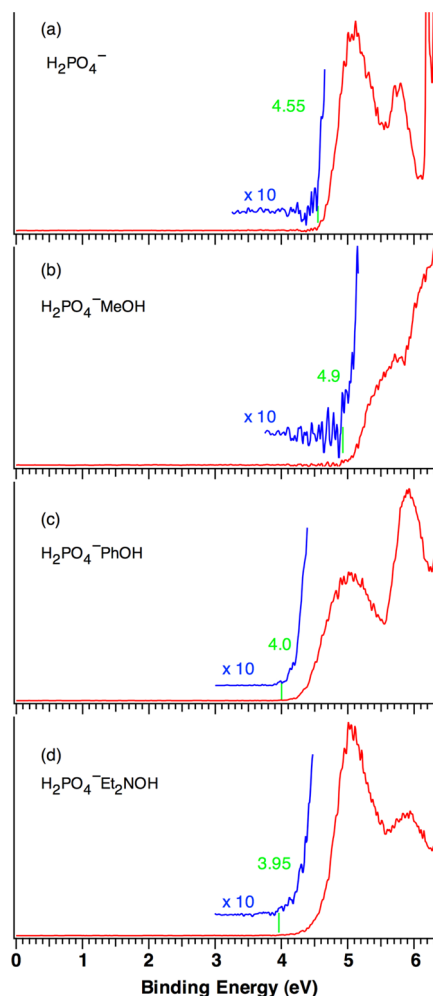


Figure 3. Photoelectron spectra at 20 K for H₂PO₄⁻ (a), H₂PO₄⁻ • MeOH (b), H₂PO₄⁻ • PhOH (c), and H₂PO₄⁻ • Et₂NOH (d) at 193 nm (6.424 eV). Blue inserts are blow ups (10×) of the onset region and the green lines and numbers provide the locations of the thresholds and the assigned ADEs.

detachment energies (which correspond to the transition from the ground electronic state of the anion to the ground electronic state of the neutral) are obtained from the peak maximum of the lowest energy band and are given in Table 2. All of these values are well reproduced by the M06-2X computations in that the average error (0.09 eV) is within the estimated experimental uncertainty of 0.1 eV, and the largest discrepancy is 0.2 eV. As for the ADEs, upper limits for these quantities were determined from the onset regions of the spectra and are given at the point where the signal is reliably above the background. This was done because photoelectron spectroscopy is a vertical process, and when there is a large geometry change between an anion and its corresponding neutral, as is the case here, then the observed threshold will be larger than that for the thermodynamic value.²¹ The assigned upper limits to the ADEs in this work are significantly greater than the computed predictions which is expected, but the former values still are up to 0.6 eV *smaller* than those for the free anions! This indicates that when ΔBDE is large, hydrogen transfer occurring on the neutral surface can significantly

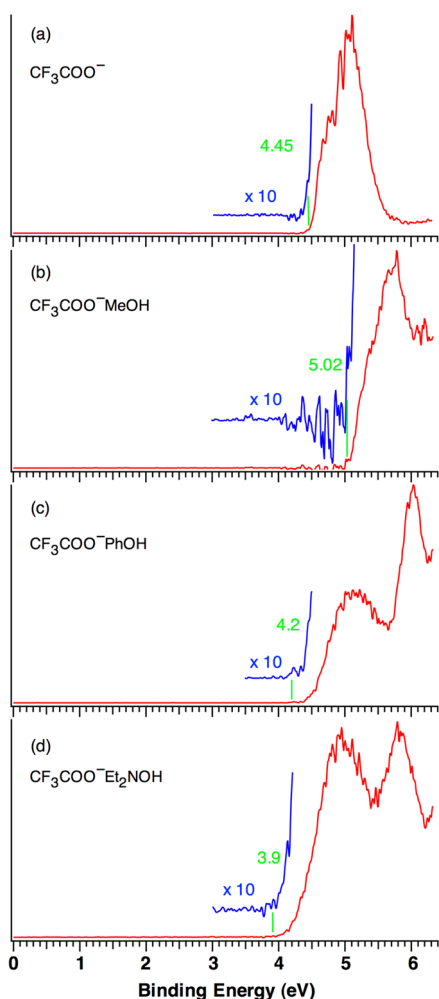


Figure 4. Photoelectron spectra at 20 K for CF_3CO_2^- (a), $\text{CF}_3\text{CO}_2^- \bullet \text{MeOH}$ (b), $\text{CF}_3\text{CO}_2^- \bullet \text{PhOH}$ (c), and $\text{CF}_3\text{CO}_2^- \bullet \text{Et}_2\text{NOH}$ (d) at 193 nm (6.424 eV). Blue inserts are blow ups (10 \times) of the onset region and the green lines and numbers provide the locations of the thresholds and the assigned ADEs.

reduce the thermodynamic requirements to remove electrons from anionic complexes and provides an additional driving force for electron transfer.

When an electron is formally lost from the anionic partner in $\text{A}^- \bullet \text{HX}$, a hydrogen atom transfer takes place on the neutral surface to afford $\text{AH} \bullet \text{X}^\bullet$. In contrast, a proton transfer occurs when the electron is removed from HX. One might naively assume that the electron comes from the anion center of the complex since negative ions are typically much easier to oxidize than neutral compounds. However, in the cluster anion the neutral partner HX raises the ADE of A^- in the absence of a concomitant hydrogen shift, whereas the ionic component lowers the ionization energy of the acid. An alternative pathway involving proton transfer in the anion cluster followed by electron detachment leads to the same thermodynamic conclusion. It appears to be unlikely, however, because weak bases were selected to disfavor $\text{HA} \bullet \text{X}^-$ structures and photodetachment is a vertical process so that the neutral species are initially formed with the same geometries as their cold (20 K) anionic precursors. Thermodynamics of course says nothing about the pathway and the photoejected electron need not come from A^- or HX. That is, a delocalized electron from the cluster ion as a whole maybe lost.

To address this issue further, spin densities of the radical complexes with the optimized geometries of the anions were examined. Upon the basis of these results, both limiting processes were found to take place. That is, the electron is lost predominately from A^- in the methanol clusters (i.e., 93 and 74% of the spin is on the H_2PO_4 and CF_3CO_2 fragments, respectively), and from HX in the two phenol complexes (i.e., 99 and 100% of the unpaired electron is located on the phenol moiety of the H_2PO_4 and CF_3CO_2 clusters, respectively). In accord with these computational predictions, the experimental ionization energy for MeOH is 2.35 eV larger than for PhOH (i.e., 10.84 vs 8.49 eV).²² These two pathways are limiting extremes, nevertheless, as the electron can be lost from the system as a whole and the unpaired electron can be delocalized over the entire cluster. This is the case for the dimethylhydroxylamine species where 41 and 28% of the unpaired electron is found to reside on the H_2PO_4 and CF_3CO_2 fragments, respectively (Figure 5). Proton coupled electron detachment is

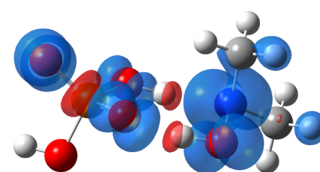


Figure 5. Spin densities of $\text{H}_2\text{PO}_4 \bullet \text{Me}_2\text{NOH}$ with isovalues of $0.002 \text{ e}^- \text{ \AA}^{-3}$.

just one of two extreme avenues for the migration of a hydrogen, and though this work only deals with the oxidation portion of redox reactions undergoing proton coupled electron transfer, there are obvious parallels between the two processes.^{23–25}

CONCLUSIONS

Hydrogen bonds can activate compounds toward oxidation if a hydrogen relocates upon the loss of an electron. Computations and photoelectron spectra of $\text{A}^- \bullet \text{HX}$ clusters where $\text{A}^- = \text{H}_2\text{PO}_4^-$ and CF_3CO_2^- and $\text{HX} = \text{CH}_3\text{OH}$, PhOH, and $(\text{CH}_3)_2\text{NOH}$ or $(\text{CH}_3\text{CH}_2)_2\text{NOH}$ indicate that adiabatic electron detachment energies can be diminished relative to the values for A^- by 0.47–1.87 eV or 11–43 kcal mol⁻¹. Two limiting pathways for these rearrangements on the neutral surface are hydrogen atom and proton transfers depending upon where the electron is lost from the ionic cluster. Given that electrons are quantum mechanical in nature and that the unpaired electron can be delocalized over the entire complex, a continuum of processes can be envisioned much like variable E2 transition structures, which can have varying amounts of E1_{cb} and E1 character.

ASSOCIATED CONTENT

Supporting Information

Calculated structures and energies, and the complete citation to ref 12 are provided. This material is available free of charge via the Internet at <http://pubs.acs.org>.

AUTHOR INFORMATION

Corresponding Authors

kass@umn.edu

xuebin.wang@pnnl.gov

Notes

The authors declare no competing financial interest.

■ ACKNOWLEDGMENTS

Generous support from the National Science Foundation, and the Minnesota Supercomputer Institute for Advanced Computational Research are gratefully acknowledged. The photoelectron spectra work was supported by the U.S. Department of Energy (DOE), Office of Science, Office of Basic Energy Sciences, Division of Chemical Sciences, Geosciences & Biosciences, and was performed at EMSL, a national scientific user facility sponsored by DOE's Office of Biological and Environmental Research and located at Pacific Northwest National Laboratory, which is operated by Battelle for DOE.

■ REFERENCES

- (1) Meot-Ner, M. *Chem. Rev.* **2012**, *112*, PR22–PR103.
- (2) (a) Hierl, P. M.; Ahrens, A. F.; Henschman, M.; Viggiano, A. A.; Paulson, J. F.; Clary, D. C. *J. Am. Chem. Soc.* **1986**, *108*, 3142–3143. (b) Bogdanov, B.; McMahon, T. B. *Int. J. Mass Spectrom.* **2005**, *241*, 205–223.
- (3) Bartmess, J. E. *NIST Chemistry WebBook, NIST Standard Reference Database Number 6*; Mallard, W. G., Lustrum, P. J., Eds.; National Institute of Standards and Technology: Gaithersburg, MD, 2011; <http://webbook.nist.gov>.
- (4) Li, R.-Z.; Liu, C.-W.; Gao, Y. Q.; Jiang, H.; Xu, H.-G.; Zheng, W.-J. *J. Am. Chem. Soc.* **2013**, *135*, 5190–5199.
- (5) Castleman, A. W., Jr.; Bowen, K. H., Jr. *J. Phys. Chem.* **1996**, *100*, 12911–12944.
- (6) Beletskiy, E. V.; Schmidt, J.; Wang, X.-B.; Kass, S. R. *J. Am. Chem. Soc.* **2012**, *134*, 18534–18537.
- (7) Wang, X.-B.; Wang, L.-S. *Rev. Sci. Instrum.* **2008**, *79*, 073108.
- (8) Arnold, D. W.; Bradforth, S. E.; Kim, E. H.; Neumark, D. M. *J. Chem. Phys.* **1995**, *102*, 3493–3509.
- (9) Wang, X.-B.; Wang, Y.-L.; Yang, J.; Xing, X.-P.; Li, J.; Wang, L. S. *J. Am. Chem. Soc.* **2009**, *131*, 16368–16370.
- (10) (a) Zhao, Y.; Truhlar, D. G. *J. Phys. Chem. A* **2008**, *112*, 1095–1099. (b) Zhao, Y.; Truhlar, D. G. *Theor. Chem. Acc.* **2008**, *120*, 215–241. (c) Zhao, Y.; Truhlar, D. G. *Acc. Chem. Res.* **2008**, *41*, 157–167.
- (11) Dunning, T. H., Jr. *J. Chem. Phys.* **1989**, *90*, 1007–1023.
- (12) Frisch, M. J.; Trucks, G. W.; Schlegel, H. B.; Scuseria, G. E.; Robb, M. A., et al. *Gaussian 09*; Gaussian, Inc.: Wallingford CT, 2009.
- (13) (a) Hampel, C.; Peterson, K.; Werner, H.-J. *Chem. Phys. Lett.* **1992**, *190*, 1–12. (b) Deegan, M. J. O.; Knowles, P. J. *Chem. Phys. Lett.* **1994**, *227*, 321–326. (c) Knowles, P. J.; Hampel, C.; Werner, H.-J. *J. Chem. Phys.* **1993**, *99*, 5219–5227; *erratum: J. Chem. Phys.* **2000**, *112*, 3106.
- (14) Wang, X.-B.; Vorpapel, E. R.; Yang, X.; Wang, L.-S. *J. Phys. Chem. A* **2001**, *105*, 10468–10474.
- (15) Angel, L. A.; Ervin, K. M. *J. Phys. Chem. A* **2006**, *110*, 10392–10403.
- (16) Gunion, R. F.; Gilles, M. K.; Polak, M. L.; Lineberger, W. C. *Int. J. Mass Spectrom. Ion Processes* **1992**, *117*, 601–620.
- (17) Ervin, K. M.; DeTuri, V. F. *J. Phys. Chem. A* **2002**, *106*, 9947–9956.
- (18) Nee, M. J.; Osterwalder, A.; Zhou, J.; Neumark, D. M. *J. Chem. Phys.* **2006**, *125*, 014306.
- (19) Fu, Y.; Yu, T.-Q.; Wang, Y.-M.; Liu, L.; Guo, Q.-X. *Chin. J. Chem.* **2006**, *24*, 299–306.
- (20) Luo, Y.-R. *Handbook of Bond Dissociation Energies in Organic Compounds*; CRC Press: Boca Raton, FL, 2003; pp 380.
- (21) Giles, M. K.; Ervin, K. M.; Ho, J.; Lineberger, W. C. *J. Phys. Chem.* **1992**, *96*, 1130–1141.
- (22) Lias, S. G.; Rosenstock, H. M.; Draxl, K.; Steiner, B. W.; Herron, J. T.; Holmes, J. L.; Levin, R. D.; Liebman, J. F.; Kafafi, S. A. *NIST Chemistry WebBook, NIST Standard Reference Database Number 6*;

Mallard, W. G., Lustrum, P. J., Eds.; National Institute of Standards and Technology: Gaithersburg, MD, 2011; <http://webbook.nist.gov>.

(23) Warren, J. J.; Tronic, T. A.; Mayer, J. M. *Chem. Rev.* **2010**, *110*, 6971–7001.

(24) Usharani, D.; Lacy, D. C.; Borovik, A. S.; Shaik, S. *J. Am. Chem. Soc.* **2013**, *135*, 17090–17104.

(25) Westlake, B. C.; Brennaman, M. K.; Concepcion, J. J.; Paul, J. J.; Bettis, S. E.; Hampton, S. D.; Miller, S. A.; Lebedeva, N. V.; Forbes, M. D. E.; Moran, A. M.; Meyer, T. J.; Papanikolas, J. M. *Proc. Natl. Acad. Sci. U.S.A.* **2011**, *108*, 8554–8558.